

Available online at [www.sciencedirect.com](http://www.sciencedirect.com)

ScienceDirect

journal homepage: [www.elsevier.com/locate/he](http://www.elsevier.com/locate/he)

# Activity of varying compositions of Co–Ni–P catalysts for the methanolysis of ammonia borane

Kehinde O. Amoo<sup>a</sup>, Edith N. Onyeozili<sup>b</sup>, Egwu E. Kalu<sup>c,\*</sup>,  
James A. Omoleye<sup>a</sup>, Vincent E. Efevbokhan<sup>a</sup>

<sup>a</sup> Department of Chemical Engineering, Covenant University, Km 10, Idiroko Road, Canaan Land, Ota, Nigeria

<sup>b</sup> Department of Chemistry, Florida A&M University, Tallahassee, FL 32307, USA

<sup>c</sup> Dept. of Chemical & Biomedical Engineering, Florida A&M Univ. and Florida State Univ., Tallahassee, FL 32310, USA

## ARTICLE INFO

### Article history:

Received 10 June 2016

Received in revised form

23 August 2016

Accepted 24 August 2016

Available online xxx

### Keywords:

Cobalt

Nickel

Methanolysis

Ammonia-borane

Electroless

Langmuir–Hinshelwood

## ABSTRACT

Various compositions of Co–Ni–P catalysts supported on a palladium-activated  $\text{Al}_2\text{O}_3$  (Pd– $\text{Al}_2\text{O}_3$ ) substrate were synthesized, characterized and investigated for catalytic methanolysis of ammonia-borane (AB,  $\text{H}_3\text{NBH}_3$ ). The Co–Ni–P/Pd– $\text{Al}_2\text{O}_3$  catalysts were synthesized by polymer-stabilized Pd nanoparticle-catalyzed and activation of the  $\text{Al}_2\text{O}_3$  substrate support and the electroless deposition of cobalt-nickel (Co–Ni) metal particles on the surface of the  $\text{Al}_2\text{O}_3$  support for a plating time of 30 min. The Co–Ni–P/Pd– $\text{Al}_2\text{O}_3$  catalysts are stable enough to be isolated as solid materials and characterized by X-ray Diffraction (XRD), Energy Dispersive X-ray Spectroscopy (EDS) and Scanning Electron Microscopy (SEM). At  $40 \pm 0.5^\circ\text{C}$ , the isolable, re-dispersible and reusable catalysts were found active in the methanolytic dehydrogenation of ammonia-borane retaining up to 65% of its initial activity after five cycles. Rates of hydrogen evolution were used to determine the kinetics of methanolysis reaction. The ranges of examined catalyst particle amounts, AB concentrations and temperatures were 15.75–63 mg, 50–200 mM, and  $30$ – $55^\circ\text{C}$ , respectively. Hydrogen desorption was identified as the rate controlling step in the methanolysis reaction and using the data, the kinetic rate constant ( $k_{\text{H}_2}$ ), the hydrogen desorption equilibrium constant ( $K_{\text{H}_2}$ ), and the overall equilibrium constant ( $K_1$ ) parameters in a Langmuir–Hinshelwood rate expression were determined to be 1.4 mol/g-cat. s, 1.5918 L/mol and 1.5986 L/mol, respectively. Activation parameters such as enthalpy of activation ( $\Delta H$ ), entropy of activation ( $\Delta S$ ), and activation energy ( $E_a$ ) that were obtained by Eyring and Arrhenius equations are reported for the various catalyst ratios.

© 2016 Hydrogen Energy Publications LLC. Published by Elsevier Ltd. All rights reserved.

## Introduction

In order to achieve the envisioned hydrogen economy of the future, major improvements in the prevailing technologies for the production, storage, and usage of hydrogen gas are

needed. In recent years, intensive efforts have been devoted to developing safe and efficient methods for hydrogen storage. The chemical hydrogen storage, in which hydrogen is stored in chemical hydrides such as  $\text{NaBH}_4$ ,  $\text{H}_3\text{NBH}_3$ ,  $\text{LiH}$ ,  $\text{NaH}$ ,  $\text{CaH}_2$ ,  $\text{MgH}_2$ ,  $\text{LiAlH}_4$ , etc. and released via an irreversible chemical reaction, is a promising strategy. Among the chemical

\* Corresponding author.

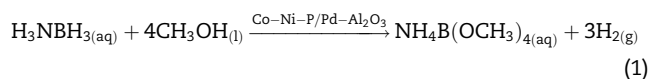
E-mail addresses: [EEK4012@fsu.edu](mailto:EEK4012@fsu.edu), [egwu.kalu@famu.edu](mailto:egwu.kalu@famu.edu), [EEK4012@gmail.com](mailto:EEK4012@gmail.com) (E.E. Kalu).

<http://dx.doi.org/10.1016/j.ijhydene.2016.08.164>

0360-3199/© 2016 Hydrogen Energy Publications LLC. Published by Elsevier Ltd. All rights reserved.

hydrides, ammonia borane ( $\text{NH}_3\text{BH}_3$ ) (AB) with 19.6 wt. % hydrogen content is one of the most promising hydrogen storage materials that exceed the 2015 target of U.S. Department of Energy (9 wt% hydrogen content) requirement for a material to be practically applicable for hydrogen storage. In addition, AB is relatively non-toxic and has high stability [1]. Generally, the liberation of hydrogen stored in AB can be achieved through either thermal degradation in solid state at above 70 °C or solvolysis (hydrolysis or methanolysis) in liquid phase under mild conditions [2–4]. Over the years a lot of research work has gone into the hydrolysis of AB, Kang et al. [5] and Wang et al. [6] studied the effect of bimetallic nanoparticles supported on carbon nanotubes as catalysts for the hydrolysis of AB; both studies showed great and promising catalytic hydrolytic activity. Alternatively, trimetallic nanoparticles which were synthesized on carbon nanotubes support and also the in situ method [7,8] for the dehydrogenation of AB exhibited superior catalytic activity in comparison to the studies in Refs. [5,6].

However, the hydrolysis of ammonia borane in concentrated solutions, in addition to producing hydrogen, can cause liberation of ammonia gas in small quantities that would pose a problem in fuel cell applications. In addition, the hydrolysis of AB yields a by-product that contains B–O bonds that are difficult to reduce and making the by-product not readily recyclable [4]. A recent study [2] in which transition metal chlorides ( $\text{RuCl}_3$ ,  $\text{RhCl}_3$ ,  $\text{PdCl}_2$ , and  $\text{CoCl}_2$ ) were used as catalysts has shown that both problems can be eliminated by using methanol as solvent instead of water, yielding hydrogen gas and ammonium tetramethoxyborate. Unlike AB hydrolysis by-product, the methanolysis by-product (ammonium tetramethoxyborate) can be recycled into ammonia-borane by a room temperature process with  $\text{LiAlH}_4$  in addition to  $\text{NH}_4\text{Cl}$ . Similar to hydrolysis reaction, the methanolysis of ammonia-borane can release up to 3.0 stoichiometric equivalents of  $\text{H}_{2(g)}$  per mole of ammonia-borane with a suitable catalyst and the reaction can be represented as in Eq. (1):



Several transition metal catalysts, their oxides and alloys have been studied for the methanolysis of ammonia-borane for hydrogen generation. Amongst these, the noble-metal catalysts, such as palladium(0) [10], ruthenium(0) [9,11] and rhodium(0) nanoparticles [9,12], have been identified as highly active for the process. However, because of their high costs, less expensive options – especially from the first row transition metal group – have led to the consideration of non-noble metal catalysts such as Nickel (Ni), Iron (Fe) and Cobalt (Co) [13–20], either singly or in combination with a noble-metal catalyst. Sun et al. [21] used 7 nm CoPd nanoparticles on carbon support with catalyst composition  $\text{Co}_{48}\text{Pd}_{52}$  showing the highest activity. On the other hand, Kalindi et al. [22] examined in-situ generated and non-supported Co–B, Ni–B and Co–Ni–B for the methanolysis of ammonia borane and found that Co–Ni–B showed greater catalytic activity towards methanolysis of AB compared to the individual metal–metal borides. The Co–Ni catalyst they evaluated was not supported and interest to evaluate the catalytic activity of supported

Co–Ni composite for the methanolysis of AB led to the current evaluation of electrolessly deposited Co–Ni–P for AB methanolysis. Although transition metal nanoparticles are significant in the methanolysis of ammonia-borane, they have tendency to agglomerate resulting in the catalysts having a relatively short lifetime [23]. Microporous or mesoporous materials as well as oxide supports with large surface area can be used to ameliorate nanoparticle aggregation while maintaining large surface area, high activity, and long lifetime for the catalyst [24]. The use of the first row transition metals as catalysts for methanolysis of AB for hydrogen generation will lead to the development of low-cost and efficient catalysts that may result in the development of a low cost energy gas source for fuel cells.

This work reports the synthesis, characterization, and the use of various compositions of the Co–Ni–P catalyst supported on palladium-activated  $\text{Al}_2\text{O}_3$  (Co–Ni–P/Pd– $\text{Al}_2\text{O}_3$ ) as a highly cost effective, very active and reusable catalyst for the generation of hydrogen from the methanolysis of AB. The Co–Ni–P/Pd– $\text{Al}_2\text{O}_3$  catalyst was prepared by first mixing  $\text{Al}_2\text{O}_3$  with Pd-catalyst ink solution, subjecting the mixture to high temperature to activate the  $\text{Al}_2\text{O}_3$  for electroless deposition and followed by the electroless deposition of Co–Ni–P. The prepared Co–Ni–P/Pd– $\text{Al}_2\text{O}_3$  catalyst was isolated from the electroless bath as solid nanoparticles material and characterized by XRD, EDS, and SEM. The kinetics of the catalytic methanolysis reaction was studied by measuring the volume of evolved hydrogen gas over varying catalysts amount, AB substrate concentration, and temperature. A Langmuir–Hinshelwood (LH) kinetic mechanism model was developed to interpret the kinetic data with the parameters (surface kinetic rate constant ( $k_{\text{H}_2}$ ), the hydrogen desorption equilibrium constant ( $K_{\text{H}_2}$ ), and the overall equilibrium constant ( $K_1$ )) determined using MATLAB® inbuilt algorithm, *fsolve*, for a system of nonlinear equations. This study shows that the Co–Ni–P/Pd– $\text{Al}_2\text{O}_3$  catalyst can be considered as low cost, very effective, and reusable catalyst in the methanolysis of ammonia-borane to generate hydrogen gas.

## Experimental

### Chemicals

Methanol (99.8%), ethanol (99.5%), palladium (II) acetate (98%), potassium D-gluconate (99%), nickel (II) sulphate hexahydrate (99%), borane-ammonia complex (97%), and cobalt (II) sulphate heptahydrate (99%) were all purchased from Sigma–Aldrich Co (St. Louis, MO), while potassium sodium tartrate tetrahydrate (99%) and aluminium oxide (98.5%) were purchased from BDH chemical Eng. Co. and Baker & Adamson Co., respectively. Sodium hypophosphite monohydrate (98%) and ammonium hydroxide (99%) were purchased from J.T. Baker Co. (USA). PVB Butvar B-79 was supplied by Solutia Inc. (St. Louis, MO).

### Preparation of the Co–Ni–P/Pd– $\text{Al}_2\text{O}_3$ catalyst

The Co–Ni–P catalyst was prepared and supported on Pd– $\text{Al}_2\text{O}_3$  by using electroless deposition method. Cobalt (II)

sulphate heptahydrate and nickel (II) sulphate hexahydrate were used as the source of cobalt and nickel, respectively. Potassium D-gluconate, a source of gluconic acid was used as the complexing agent to control the rate of release of free metal ion for the reduction reaction. Sodium hypophosphite was used as the reducing agent, and also served as the source of phosphorus in the catalyst deposit. Potassium sodium tartrate tetrahydrate was used as a chelating agent. Additionally, ammonium hydroxide was added to adjust the pH of the electroless bath solution. During plating process, the bath was maintained at specific temperatures as shown in Table 1. The Co–Ni–P/Pd–Al<sub>2</sub>O<sub>3</sub> catalysts with different amounts of cobalt and nickel deposited were prepared by varying the metallic weight amounts of CoSO<sub>4</sub> and NiSO<sub>4</sub> in six (6) different electroless bath solutions and designated as Co–Ni (100:0), Co–Ni (86.4:13.6), Co–Ni (66.7:33.3), Co–Ni (50:50), Co–Ni (33.3:66.7), and Co–Ni (0:100), respectively. The bath composition and operating conditions used for the preparation of the electroless Co–Ni–P alloy deposits are shown in Table 1.

The electroless deposition of Co–Ni–P alloy requires an activated surface to initiate the deposition process. For that reason, the aluminium oxide support surface was made catalytically active employing a previously reported method [25,26]. A measured amount of poly-vinyl-butylal (PVB) (Solutia Inc. Butvar B-79) i.e. (22 g) was dissolved in 140 cm<sup>3</sup> of ethanol. 0.2 g of palladium acetate [Pd(CH<sub>3</sub>CO<sub>2</sub>)<sub>2</sub>]<sub>2</sub> (47.05% Pd) was dissolved in a few drops (~2 cm<sup>3</sup>) of ammonium hydroxide (NH<sub>4</sub>OH). The dissolved [Pd(CH<sub>3</sub>CO<sub>2</sub>)<sub>2</sub>]<sub>2</sub>/(NH<sub>4</sub>OH) mixture was then added to a 44 g ethanol-poly(vinyl) butylal mixture and stirred continuously for 18 h. The resulting mixture was thereby referred to as the Pd-Catalyst Ink. In order to make the Al<sub>2</sub>O<sub>3</sub> active for electroless deposition, a known amount of the Pd-Catalyst Ink (6.7 g) was mixed with 10 g of Al<sub>2</sub>O<sub>3</sub>. The Pd-Catalyst Ink was then mixed thoroughly with the measured amount of Al<sub>2</sub>O<sub>3</sub> until all the particles were thoroughly covered with the Pd-Ink. The mixture was then allowed to dry at room temperature (28 °C) for approximately 3 h. The dried/caked mixture was placed in the furnace at a temperature of 450 °C for a period of 24 h.

To initiate the electroless deposition process, 1.0 g of activated aluminium oxide (Pd–Al<sub>2</sub>O<sub>3</sub>) support was placed in 200 mL of the electroless plating bath solution and the electroless Co–Ni–P particle deposition conducted for 30 min. The solutions were thoroughly mixed using a stirrer at a constant speed of 1000 rpm such that the Co–Ni particles were evenly deposited on the surface of the substrate support. After plating, the resulting coated Pd–Al<sub>2</sub>O<sub>3</sub>/Co–Ni–P catalysts

were filtered and washed with deionized (DI) water. The plated particles were then dried in the oven at 70 °C for 12 h. After drying, the catalyst particles were tested for their magnetic properties and observed to be magnetic, which is a distinct property of cobalt and nickel metals. The magnetic intensity seemed more pronounced as amount of the cobalt metal particles increased in the Co–Ni–P/Pd–Al<sub>2</sub>O<sub>3</sub> catalysts.

#### Method to test the catalytic activity of the various Co–Ni–P/Pd–Al<sub>2</sub>O<sub>3</sub> catalysts in the methanolysis of ammonia-borane

The catalytic activity of the electrolessly deposited Co–Ni–P/Pd–Al<sub>2</sub>O<sub>3</sub> catalyst was determined through an estimation of the amount of hydrogen generated during the methanolysis of AB for a specified amount of time. The experimental set-up used in this work included a 30 mL reaction flask, a 1 L beaker filled with water acted as the water bath, plastic tubing, a Liebig condenser, a hot plate magnetic stirrer, magnetic stirrer, and a 50 mL burette. Both heating and stirring occurred concurrently at the water bath and reaction flask through the hot plate magnetic stirrer (Thermo Scientific Ceramic Hot Plate Magnetic Stirrer). In all experiments, the reaction flask (30 mL) was placed in the water bath wherein the temperature was kept constant at the specified temperature ranges. Then, the graduated burette (50 mL) filled with water was connected to the reaction flask so as to measure the volume of the hydrogen gas liberated from the reaction. Basu et al. [27] stated in their previous work that the experimental error of the water-displacement method for estimating the amount of hydrogen gas evolved was estimated to be ±0.7%, buttressing the reliability of the method. Subsequently, 31.5 mg (1.0 mmol, 100 mM) AB was dissolved in 10 mL of methanol and transferred into the reaction flask and maintained at specific temperature ranges. Next, certain amounts of the Co–Ni–P/Pd–Al<sub>2</sub>O<sub>3</sub> catalyst were added into the reaction flask. The reaction was started by closing the flask and turning on the magnetic stirrer at a rotation speed of 1000 rpm (Fig. 1). The volume of hydrogen gas evolved was measured by recording the displacement of water level from the graduated burette as the reaction advanced.

#### Effect of nickel composition

The effect of the amount of nickel on the overall activity of the Co–Ni–P/Pd–Al<sub>2</sub>O<sub>3</sub> catalysts was also studied in this work. We hypothesize a Co–Ni composition with catalytic activity close to that of pure cobalt but less expensive than pure cobalt. To

**Table 1 – Composition of different electroless Co–Ni–P bath solutions.**

Material	Quantity (g/250 ml)					
	50:50	100:0	0:100	33.3:66.7	66.7:33.3	86.4:13.6
Sodium Hypophosphite	2.5	2.5	2.5	2.5	2.5	2.5
Gluconic acid	3.75	3.75	3.75	3.75	3.75	3.75
Sodium Tartrate	2.5	2.5	2.5	2.5	2.5	2.5
Nickel sulphate	1.75	0	1.75	1.75	0.875	0.48
Cobalt sulphate	1.75	1.75	0	0.875	1.75	3.02
pH	9.2–9.8	9.2–9.8	8.8–9.5	9.2–9.8	9.5–10	9.2–10
Temperature	70 ± 2 °C	70 ± 2 °C	74 ± 2 °C	72 ± 2 °C	72 ± 2 °C	70 ± 2 °C

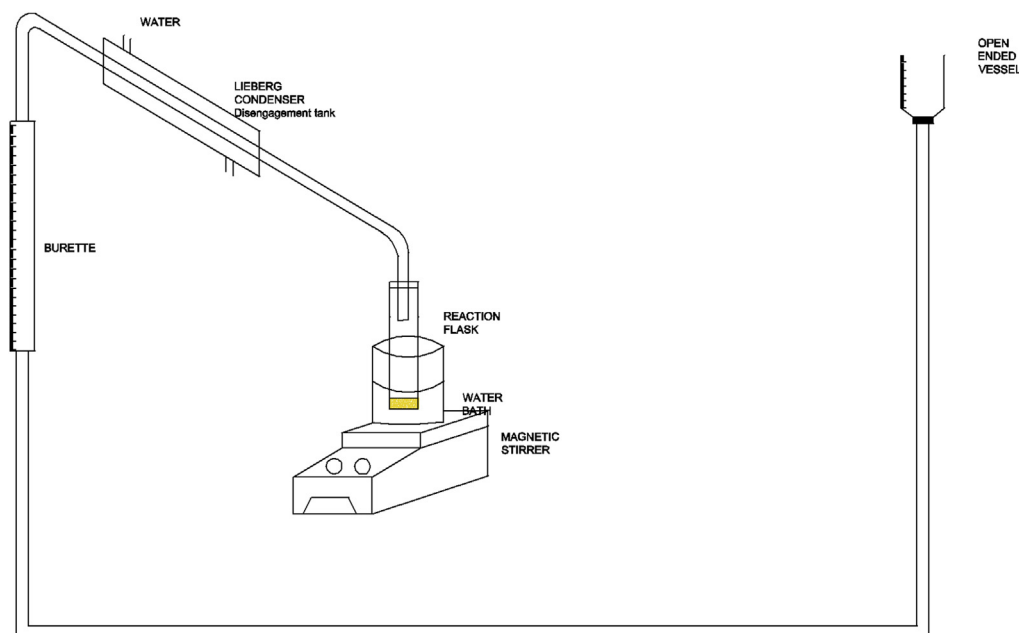


**Fig. 1 – Schematic of experimental set-up used for executing the catalytic methanolysis of ammonia-borane and measuring the volume of hydrogen gas liberated.**

determine the effect of nickel loading in the catalyst on the hydrogen generation rate, the catalytic activities of different Co–Ni–P/Pd–Al<sub>2</sub>O<sub>3</sub> catalyst compositions (Co–Ni (100:0), Co–Ni (86.4:13.6), Co–Ni (66.7:33.3), Co–Ni (50:50), Co–Ni (33.3:66.7), and Co–Ni (0:100)) were tested in the methanolysis of 10 mL of 100 mM aqueous AB solution. All the experiments were performed as described in [Section Method to test the catalytic activity of the various Co–Ni–P/Pd–Al<sub>2</sub>O<sub>3</sub> catalysts in the methanolysis of ammonia-borane](#) and results evaluated with respect to the catalytic activity and relative cost effectiveness due to the different amounts of Ni used.

#### **Kinetic study of methanolysis of ammonia-borane catalysed by Co–Ni–P/Pd–Al<sub>2</sub>O<sub>3</sub> catalyst**

In order to establish the rate law, reaction mechanism model and kinetic parameters for the catalytic methanolysis of H<sub>3</sub>NBH<sub>3</sub> using Co–Ni–P/Pd–Al<sub>2</sub>O<sub>3</sub> nanoparticles as catalyst, two sets of experiments were performed as described in [Section Method to test the catalytic activity of the various Co–Ni–P/Pd–Al<sub>2</sub>O<sub>3</sub> catalysts in the methanolysis of ammonia-borane](#). In the first set of experiments, the methanolysis reaction was carried out starting with a constant initial concentration of ammonia-borane of 100 mM (31.5 mg H<sub>3</sub>NBH<sub>3</sub> in 10 mL of methanol) and different initial amounts of the Co–Ni–P/Pd–Al<sub>2</sub>O<sub>3</sub> catalyst varying in the range of 15.75–63 mg (15.75, 25, 31.5, 45, 50, and 63 mg). In the second set of experiments, the Co–Ni–P/Pd–Al<sub>2</sub>O<sub>3</sub> initial catalyst amount was held constant at 31.5 mg while the H<sub>3</sub>NBH<sub>3</sub> concentration was varied in the range of 50, 100 and 200 mM (15.75, 31.5 and 63 mg, respectively). Finally, the catalytic methanolysis of AB was performed in the presence of Co–Ni–P/Pd–Al<sub>2</sub>O<sub>3</sub> nanoparticles at constant AB concentration (31.5 mg, 100 mM) and constant catalyst amount (31.5 mg,

Co–Ni–P/Pd–Al<sub>2</sub>O<sub>3</sub>) in 10 mL methanol at various temperatures ranging from 30 °C to 55 °C in order to obtain the activation energy ( $E_a$ ), enthalpy ( $\Delta H$ ) and entropy ( $\Delta S$ ).

#### **Isolability and reusability of the Co–Ni–P/Pd–Al<sub>2</sub>O<sub>3</sub> catalyst in the methanolysis of ammonia-borane**

After the catalytic methanolysis of ammonia-borane reaction was completed, the used catalyst was separated from the solution through filtration, washed thoroughly with deionized water and methanol, dried, and reused in the methanolysis of ammonia-borane (15.75 mg, 50 mM). A fresh equivalent of aqueous AB concentration of 50 mM was always added to the reactor vessel for each reusability test. The reusability experiments were carried out at a temperature of 40 °C and repeated 5 times under atmospheric pressure.

#### **Surface characterization of the Co–Ni–P/Pd–Al<sub>2</sub>O<sub>3</sub> catalyst**

The identification of surface properties such as catalyst crystallinity, particle sizes, morphology, and composition is relevant in understanding the role of the catalyst in the catalytic methanolysis of ammonia-borane. Powder X-ray diffraction (XRD) patterns were recorded with a Siemens D-500 X-ray Diffractometer using a non-monochromated Cu K $\alpha$  radiation source with a wavelength of 1.54 nm (30 kV, 15 mA) and a diffracted beam monochromator at room temperature. Scanning for crystallinity was performed between 2 $\theta$  degrees of 20–65°. Scanning Electron Microscopy (SEM) analysis was carried out with an FEI Nova nanoSEM 400 scanning electron microscope operating at an accelerating voltage of 20 kV, equipped with an Oxford Inca energy dispersive X-ray spectroscopy (EDS) analysis detector unit in order to study the catalyst morphology and composition, respectively.



## Results and discussion

### Surface characterization of the catalyst

As prepared catalyst was used in the methanolysis of AB and the evolution of hydrogen monitored by measuring the amount of water displaced in the burette at specified time intervals. Fig. 2 shows the plot of mole  $H_2$  evolved per mole of ammonia-borane versus time for the catalytic methanolysis of 100 mM AB in the presence of 31.5 mg Co–Ni (100:0) catalyst in 10 mL methanol at  $30 \pm 0.5^\circ C$ . No induction time was needed for the evolution of  $H_2$  gas to occur, the hydrogen evolution started immediately the methanolysis of AB was initiated and continued almost linearly until reaction was completed, producing approximately 2.3 mol of  $H_2$  which is a little shy of the theoretical 3 mol seen in Eq. (1). This disparity could be due to the remainder of  $H_2$  gas trapped in the extra amount of tubing used in the connection of the experimental setup as described in Section Method to test the catalytic activity of the various Co–Ni–P/Pd– $Al_2O_3$  catalysts in the methanolysis of ammonia-borane. The volume of hydrogen gas left unmeasured in the extra tubing was estimated to be 18.2 mL owing to the fact that the tube has an internal diameter (ID) of 0.5 cm ( $\approx 0.2$  in) and a length of 92.7 cm. Assuming an atmospheric reaction pressure and ambient temperature of 303 K, the number of moles of hydrogen to have been trapped in the tube was calculated to be 0.00067 mol. This amount of hydrogen translates to a ratio of mol  $H_2$ /mol  $NH_3BH_3$  of 0.67 mol which brings the total amount of  $H_2(g)$  liberated to approximately 2.97 mol per mole AB corroborating the 3 mol in Eq. (1). Similar to the Co–Ni (100:0) catalyst, the other catalyst compositions with increasing nickel amounts showed similar trend as the result in Fig. 2.

The compared XRD patterns of the various Co–Ni–P/Pd– $Al_2O_3$  catalysts prepared in this work are shown in Fig. 3(a) and (b), along with the  $Al_2O_3$  substrate support. The powder X-ray diffraction patterns (b – h) are identical to that of the host

$Al_2O_3$  framework lattice (a), having 6 major diffraction peaks between  $2\theta$  (deg) =  $20$ – $65^\circ$  at  $25.8^\circ$ ,  $35^\circ$ ,  $38^\circ$ ,  $43.5^\circ$ ,  $52.3^\circ$ , and  $57.8^\circ$ , matching the International Centre for Diffraction Data Pattern (ICDD Pattern 00-046-1212) for aluminium oxide. This demonstrates that the host material remains unchanged at the end of the electroless deposition procedure without observable alteration in its structure or loss in its crystallinity. The only major difference in the compared diffractograms (a–h) is the Bragg peaks at  $44.3^\circ$  and  $45.0^\circ$  as indicated by ‘★’, which is readily assignable to the presence of nickel and cobalt on the surface of the  $Al_2O_3$  support, respectively. Furthermore, there is no detectable peak attributable to the palladium nanoparticles in the compared XRD patterns in (b), most probably due to the low palladium content on the  $Al_2O_3$  support material.

An illustration of SEM study of the catalyst samples is given in Fig. 4 which shows the SEM morphology images of the electrolessly deposited Co–Ni–P/Pd– $Al_2O_3$  catalyst [Co–Ni (86.37:13.63)] particles at different magnifications. Fig. 4(a) depicts the Back Scattered Electron Diffraction SEM in Z-contrast (compositional) mode (BSED-SEM) image of the Co–Ni–P/Pd– $Al_2O_3$  catalyst of metal ratio [Co–Ni (86.37:13.63)] at  $250\times$  magnification, (b) shows the Everhart-Thornley Detector (ETD) electron image taken at  $750\times$  magnification while (c, and d) are the secondary electron images taken with the Through Lens Detector (TLD) in field immersion mode at  $7500\times$  and  $25,000\times$  magnification of the Co–Ni (86.37:13.63) catalyst, respectively. The white shining area as seen in BSED-SEM image in Fig. 4(a) indicates that the cobalt-nickel alloy of ratio 86.37:13.63 actually plated on the surface of the support. The TLD image of Fig. 4(c) invariably shows the coarse texture of the structure of the catalyst, most probably due to the Co–Ni metals deposited on the  $Al_2O_3$  substrate. The elemental chemical composition of the Co–Ni–P/Pd– $Al_2O_3$  [Co–Ni (86.37:13.63)] catalyst was studied by EDS as shown in Fig. 5.

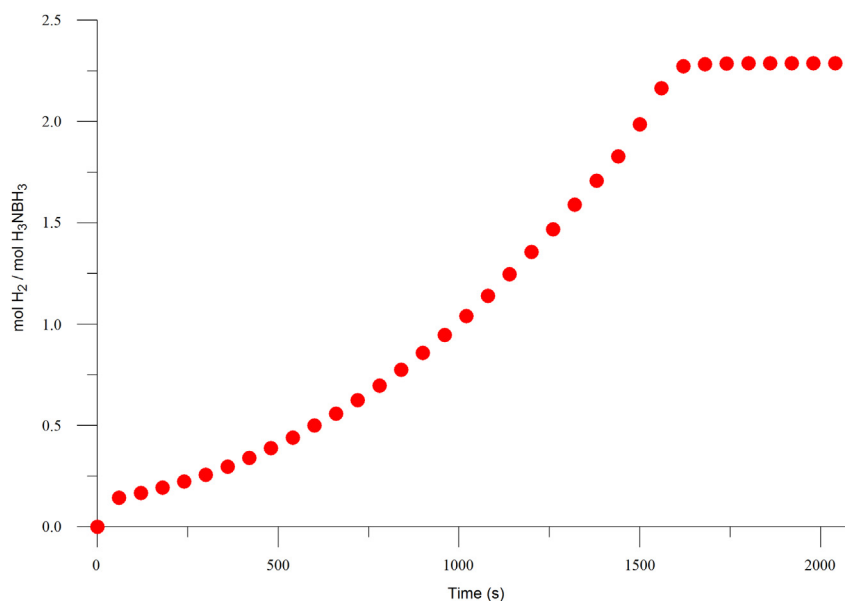


**Fig. 2** – Plot of mole  $H_2$  evolved per mole of ammonia-borane versus time (s) for the methanolysis of 100 mM AB in the presence of Co–Ni (100:0) catalyst in 10 mL methanol at  $55 \pm 0.5^\circ C$ .

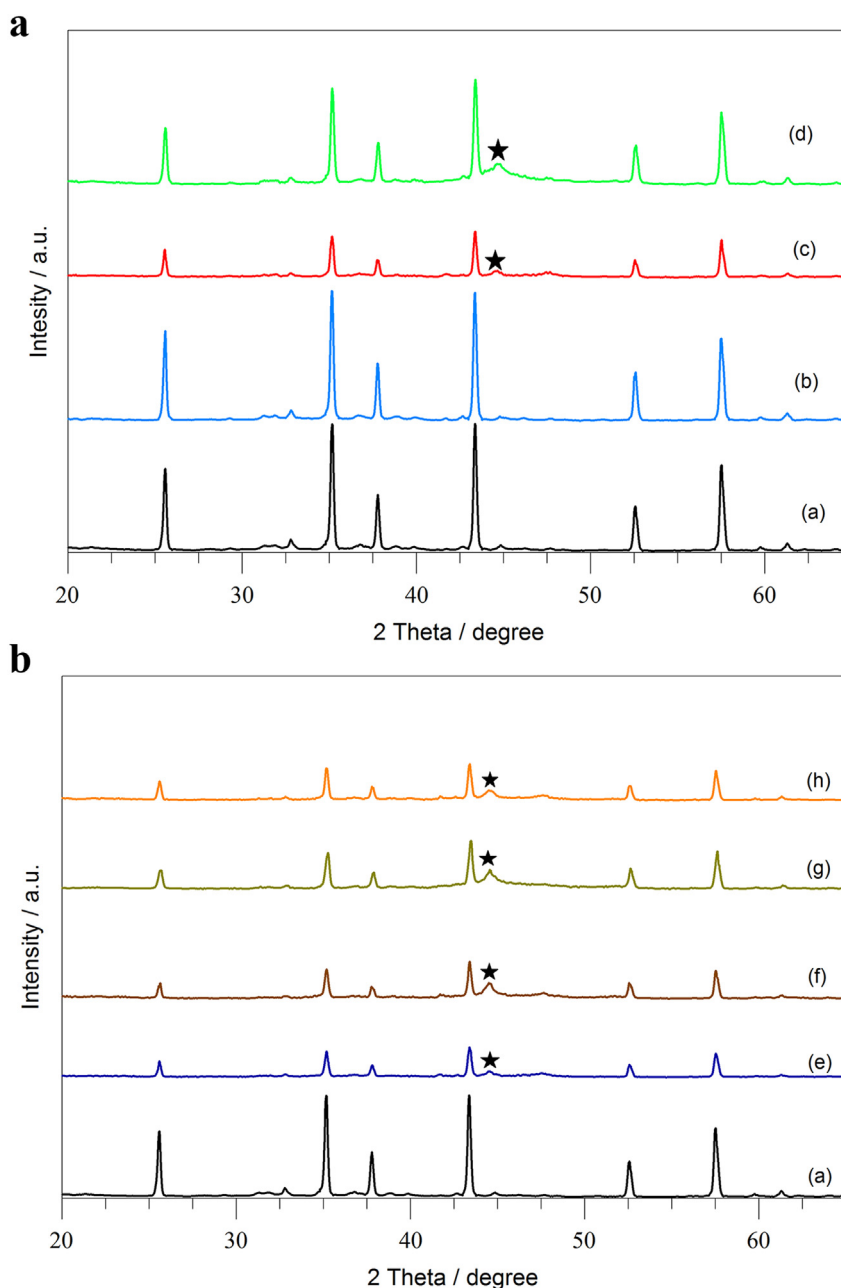


**Fig. 3 – a - The XRD Patterns of the substrate support material  $\text{Al}_2\text{O}_3$ : (a), Activated  $\text{Pd}-\text{Al}_2\text{O}_3$  (b),  $\text{Co}-\text{Ni}-\text{P}/\text{Pd}-\text{Al}_2\text{O}_3$  catalyst (100:0) (c), and  $\text{Co}-\text{Ni}-\text{P}/\text{Pd}-\text{Al}_2\text{O}_3$  catalyst (0:100) (d) all as prepared. b – The XRD Patterns of the substrate material  $\text{Al}_2\text{O}_3$  (a),  $\text{Co}-\text{Ni}-\text{P}/\text{Pd}-\text{Al}_2\text{O}_3$  catalyst (86.37:13.63) (e),  $\text{Co}-\text{Ni}-\text{P}/\text{Pd}-\text{Al}_2\text{O}_3$  catalyst (50:50) (f),  $\text{Co}-\text{Ni}-\text{P}/\text{Pd}-\text{Al}_2\text{O}_3$  catalyst (66.7:33.3) (g),  $\text{Co}-\text{Ni}-\text{P}/\text{Pd}-\text{Al}_2\text{O}_3$  catalyst (33.3:66.7) (h) all as prepared.**

A BSED image of the  $\text{Co}-\text{Ni}-\text{P}/\text{Pd}-\text{Al}_2\text{O}_3$  catalyst with 4 different compositional testing points (spectrums 1, 2, 3, and 4) is shown in Fig. 5(a) while the analogous EDS of spectrum 4 is shown in Fig. 5(b). It was found that the elements in the catalyst apart from aluminium and oxygen are cobalt, nickel and phosphorus, indicating that the  $\text{Co}-\text{Ni}-\text{P}$  metal particles indeed plated on the  $\text{Al}_2\text{O}_3$  support, in agreement with the initial elemental composition of the electroless bath. Also carbon was found in the EDS analysis due the PVB and probably SEM mount. It is to be noted that the choice of  $\text{Co}-\text{Ni}$

(86.4:13.6) catalyst whose SEM characterization properties were discussed under this section was made based on its close catalytic performance to the 100 wt. % cobalt sample (discussed below).

#### Effect of nickel composition

Generally, cobalt-based catalysts used for hydrogen generation for the methanolysis of AB are more active and more expensive than the nickel-based catalysts. Therefore, in order

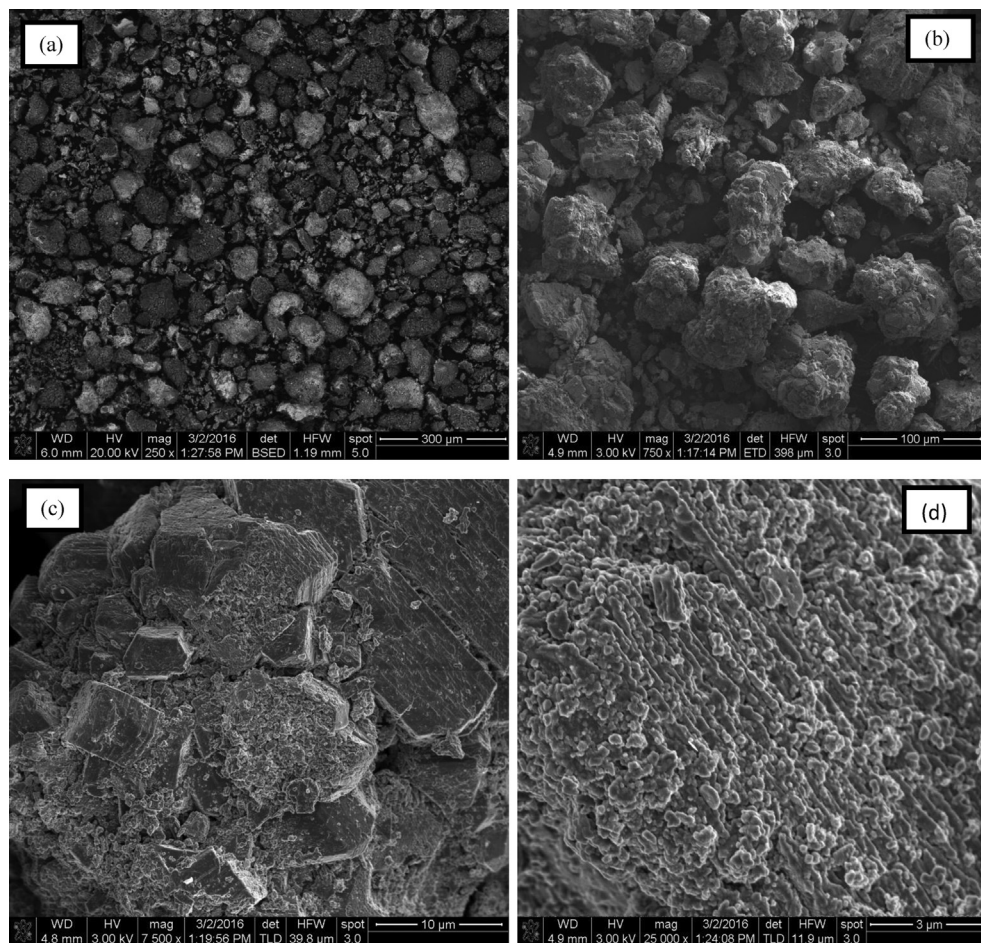


**Fig. 4 – SEM images of the Co–Ni–P/Pd–Al<sub>2</sub>O<sub>3</sub> catalyst [Co–Ni (86.37:13.63)] particles showing (a) BSED image at 250 $\times$ , (b) ETD image at 750 $\times$  and (c, d) TLD images at 7500 $\times$  and 25000 $\times$ .**

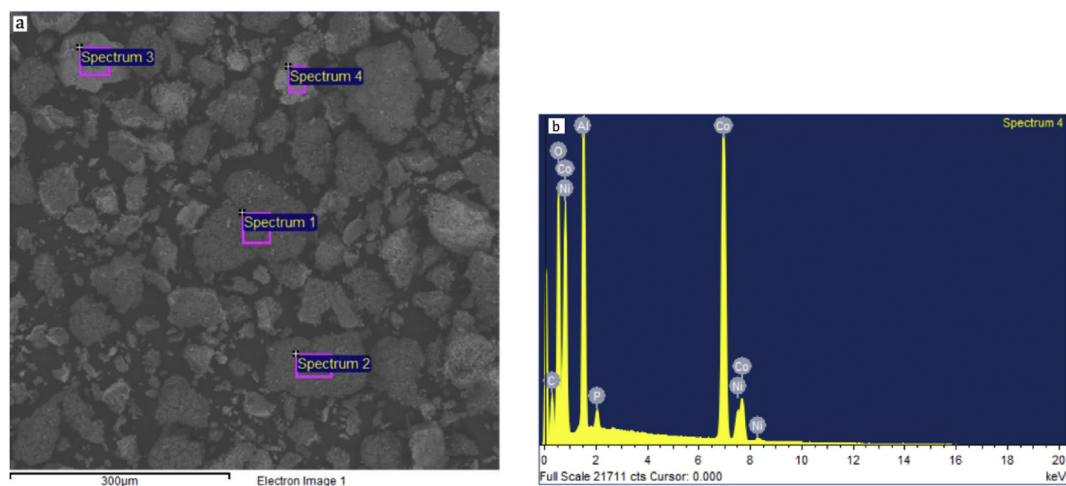


**Fig. 5 – (a) BSED image of the Co–Ni–P/Pd–Al<sub>2</sub>O<sub>3</sub> catalyst [Co–Ni (86.37:13.63)] showing the spectrums used for EDS analysis. (b) The corresponding EDS spectrum at the specified spectrum point as indicated in (a).**

to get a catalyst that has an activity close to that of the pure cobalt-plated catalyst, alloy type catalysts were prepared by varying the cobalt to nickel ratios and test their catalytic activities in the methanolysis of AB. The effect of the amount of

nickel on the overall activity of the Co–Ni–P/Pd–Al<sub>2</sub>O<sub>3</sub> catalyst was then studied. Fig. 6(a) shows that increase in the composition ratio of Nickel to Cobalt from 0 to 100 wt% resulted in a gradual decline of H<sub>2</sub>(g) (~55 mL–~16 mL)

produced at 40 °C. This observation was as expected, the rate of hydrogen generation (catalytic activity) increases with increasing amount of cobalt co-deposited with nickel. The experimental volumes of the evolved hydrogen were gotten from the methanolysis of ammonia-borane at 40 °C with a fixed mass (31.5 mg) of the cobalt-nickel catalyst of various ratios (100:0, 66.7:33.3, 50:50, 33.3:66.7, and 0:100). This was carried out to determine the mathematical correlation between the generated  $H_2$  gas at the different ratios. Since a catalyst composition that has a close activity to that of cobalt only catalyst (i.e. Co–Ni (100:0)) was required, approximately 87% (~48 mL) of the total volume of  $H_2$  (~55 mL) released from the Co–Ni (100:0) catalyst was correlated to determine the Co–Ni alloy composition. The predicted composition from the correlation (86.4:13.6) for Co–Ni was then prepared, and

experimentally confirmed, as shown in Fig. 6(b). This catalyst composition, Co–Ni (86.4:13.6) was used both for the kinetic and reusability test studies.

#### Kinetic study of methanolysis of ammonia-borane catalysed by Co–Ni–P/Pd– $Al_2O_3$ catalyst

The kinetics of the methanolysis of ammonia-borane catalysed by the Co–Ni–P/Pd– $Al_2O_3$  catalyst was studied with regard to the amount of catalyst used, amount of AB used, and temperature. The studies involved changing the amount of catalyst, ammonia-borane (AB) concentration and varying the temperature. Firstly, different amounts of the Co–Ni–P/Pd– $Al_2O_3$  (Co–Ni 86.4:13.6) catalyst nanoparticles were studied. Fig. 7 shows variation of evolved  $H_2$  as a function of

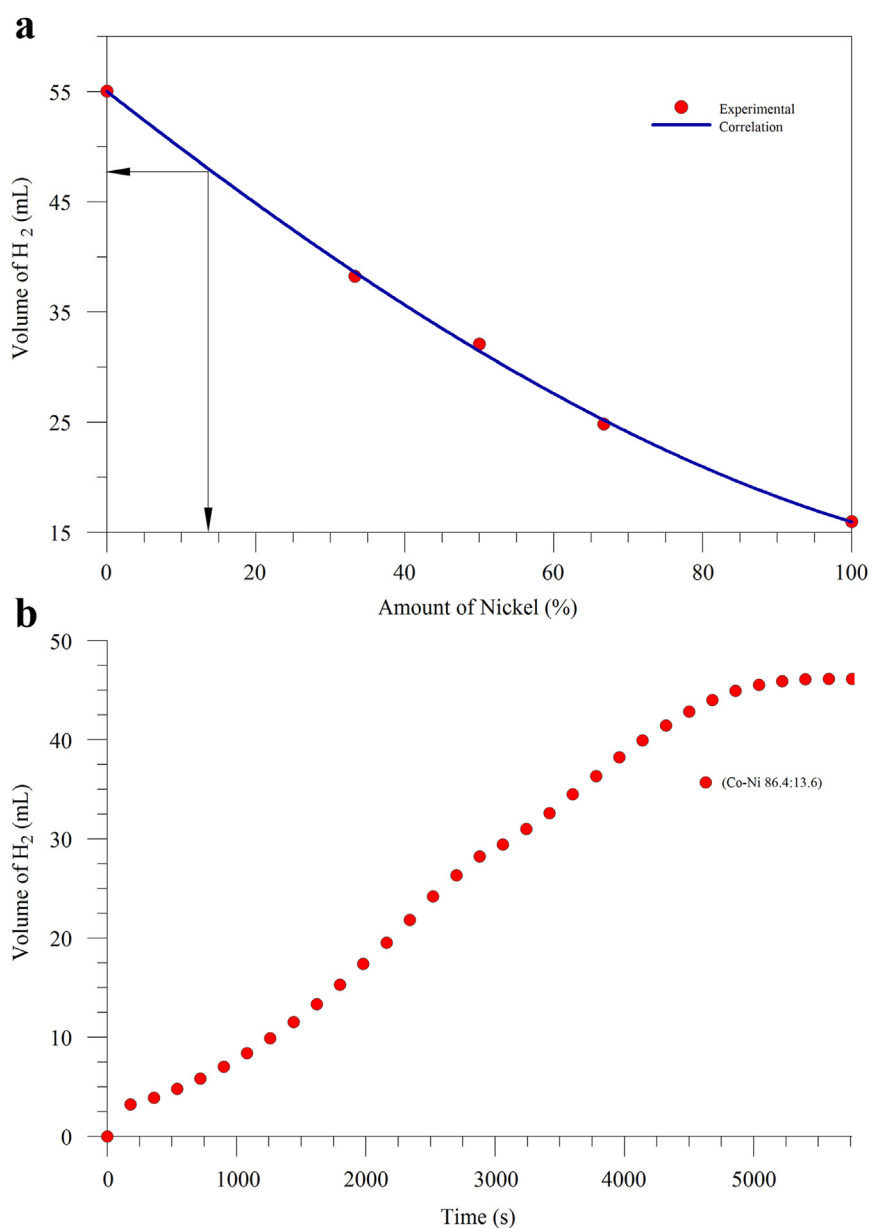


**Fig. 6 – a) Effect of Nickel amount on  $H_2$  production at  $40 \pm 0.5$  °C. b) Plot of the volume of  $H_2$  (mL) versus time (s) for the methanolysis of AB (31.5 mg, 100 mM) catalysed by Co–Ni–P/Pd– $Al_2O_3$  (Co–Ni 86.4:13.6) catalyst at  $40 \pm 0.5$  °C.**



methanolysis time at initial AB amount of 31.5 mg for different amounts of the catalyst (15.75, 25, 31.5, 45, 50 and 63 mg) at  $40 \pm 0.5$  °C. The inset in Fig. 7 is a plot of logarithmic form of the hydrogen generation rates versus the logarithmic scale of the amount of catalyst for the same reaction. This plot gives a straight line, which means that the catalytic methanolysis of ammonia-borane, catalysed by Co–Ni–P/Pd–Al<sub>2</sub>O<sub>3</sub> nanoparticles, is dependent on the amount (by weight) of the Co–Ni–P/Pd–Al<sub>2</sub>O<sub>3</sub> catalysts used as expected for a heterogeneous reaction. Hydrogen generation rate was determined by using the linear portion of each plot of ammonia-borane reaction performed with different catalyst amounts of the Co–Ni–P/Pd–Al<sub>2</sub>O<sub>3</sub> catalyst nanoparticles.

Furthermore, the effect of the H<sub>3</sub>NBH<sub>3</sub> substrate concentration on the hydrogen generation rate was studied by carrying out a series of experiments starting with various initial concentrations of AB while keeping the amount of Co–Ni–P/Pd–Al<sub>2</sub>O<sub>3</sub> catalyst constant at 31.5 mg. The plots of the volume of H<sub>2</sub> evolved versus time are depicted in Fig. 8 for the methanolysis of AB with various AB concentrations (50, 100, 200 mM), starting with a catalyst amount of 31.5 mg at  $40 \pm 0.5$  °C. The inset in Fig. 8 shows the plot of hydrogen generation rate versus AB concentration, both in logarithmic scales, which gives a straight line with the slope of  $0.0089 \approx 0$ , indicating that the catalytic methanolysis of AB catalysed by Co–Ni–P/Pd–Al<sub>2</sub>O<sub>3</sub> nanoparticles is of zeroth order with respect to ammonia borane concentration.

As a consequence of all the experimental results presented thus far, the experimental rate law for the catalytic methanolysis of AB in the presence of Co–Ni–P/Pd–Al<sub>2</sub>O<sub>3</sub> nanoparticles can be given as in Eq. (2):

$$\frac{1}{[\text{Co} - \text{Ni} - \text{P}]} \frac{3d[\text{NH}_3\text{BH}_3]}{dt} = \frac{1}{[\text{Co} - \text{Ni} - \text{P}]} \frac{d[\text{H}_2]}{dt} = k' \quad (2)$$

In previous reports on catalytic hydrolysis [28–31], and methanolysis [12,32,33] of AB, Caliskan et al. [12], Özhava et al. [32], and Peng et al. [33], assumed the catalyst particles as reactants in their analysis and expressions of the kinetic rate laws. Further, the authors did not offer any mechanistic pathway for the reactions nor the rate controlling step in the catalytic methanolysis or hydrolysis of AB. Herein, we consider the Co–Ni–P/Pd–Al<sub>2</sub>O<sub>3</sub> catalyst nanoparticles as playing the role of catalysts in the heterogeneous methanolysis reaction and derive a Langmuir–Hinshelwood (LH) kinetic mechanism model that accurately predicts the kinetic parameters during the catalytic reaction. The rate controlling step in the proposed mechanism is also provided.

Due to the fact that the catalytic methanolysis of AB is a heterogeneous catalytic reaction, the need to derive a suitable reaction mechanism for the reaction path is of utmost priority. A number of Langmuir–Hinshelwood models were developed as the rate controlling steps and tested with the experimental data obtained, including the rate law expression in Eq. (2). Only the model depicting the desorption of H<sub>2(g)</sub> as the rate-controlling step that is in agreement with the experimental data. The Langmuir–Hinshelwood model for the rate-controlling step is given in Eq. (3):

$$r_{D,H_2} = \frac{k'_{H_2} K_{H_2} C_T^3 \left[ \frac{K_1}{1} \cdot \frac{C_A C_B^4}{C_C} - C_{H_2}^3 \right]}{\left( 1 + K_A^3 C_A^3 + K_B^3 C_B^3 + K_C^3 C_C^3 + K_{H_2}^3 K_1^3 \cdot \frac{C_A C_B^4}{C_C} \right)} \quad (3)$$

Dividing the numerator and denominator of Eq. (3) by  $\left[ \frac{C_A C_B^4}{C_C} \right]$ , and with C<sub>B</sub>, (concentration of methanol) being so large relative to other species in the reacting system, the resulting equation from Eq. (3) rightly reduces to;

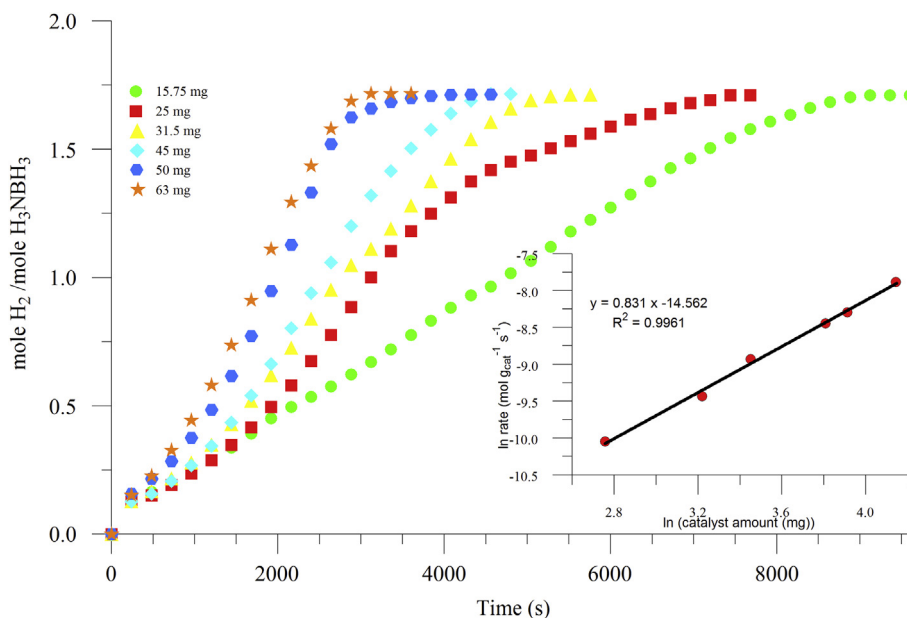


**Fig. 7** – Plot of mole H<sub>2</sub>/mole H<sub>3</sub>NBH<sub>3</sub> versus time (s) for the methanolysis of H<sub>3</sub>NBH<sub>3</sub> (31.5 mg, 100 mM) catalysed by Co–Ni–P/Pd–Al<sub>2</sub>O<sub>3</sub> catalysts with different amounts of catalyst at  $40 \pm 0.5$  °C. The inset shows the plot of the hydrogen generation rate versus the amount of catalyst (both in logarithmic scale) for the same reaction.

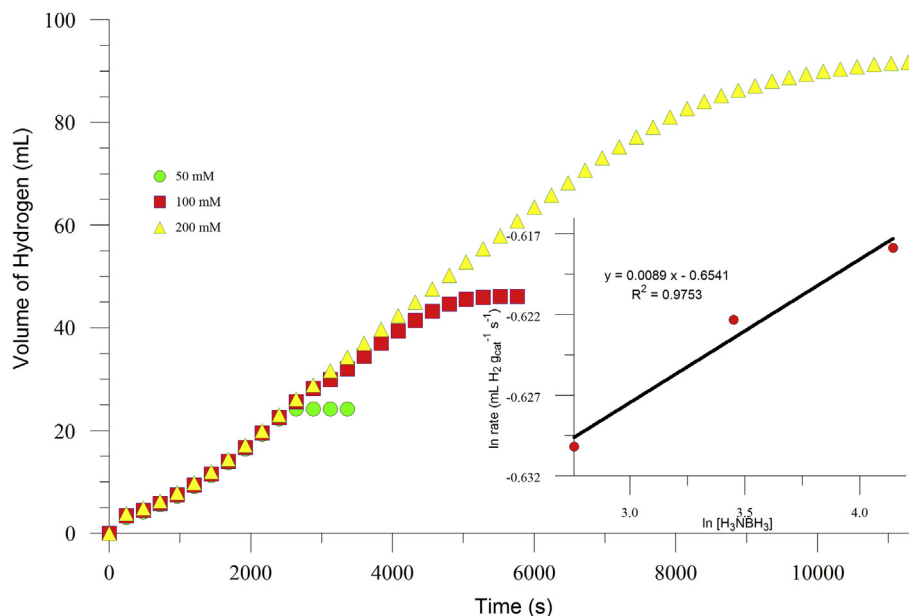


**Fig. 8** – Plot of the volume of  $\text{H}_2$  (mL) versus time (s) for the methanolysis of  $\text{H}_3\text{NBH}_3$  catalysed by Co–Ni–P/Pd– $\text{Al}_2\text{O}_3$  (31.5 mg) catalyst with different  $\text{H}_3\text{NBH}_3$  concentrations at  $40 \pm 0.5$  °C. The inset shows the plot of the hydrogen generation rate versus the concentration of AB (both in logarithmic scale) for the same reaction.

$$r_{\text{D},\text{H}_2} = \frac{\ddot{k}_{\text{H}_2}}{K_{\text{H}_2}^2 K_1} \quad (4)$$

where:

$$\ddot{k}_{\text{H}_2} = k'_{\text{H}_2} C_T^3 \quad (5)$$

Using Eq. (4), and Eq. (2) and relations between the parameters, we obtain three (3) non-linear algebraic equations that were solved to obtain the kinetic parameters ( $\ddot{k}_{\text{H}_2}$ ,  $K_{\text{H}_2}$ ,  $K_1$ ) using MATLAB® inbuilt algorithm, *fsolve*. The converged and optimized values of the respective constants are:  $\ddot{k}_{\text{H}_2} = 0.0014 \text{ mol (mg-cat)}^{-1} \text{ s}^{-1}$  (or  $1.4 \text{ mol/g-cat. s}$ ),  $K_{\text{H}_2} = 1.5918 \text{ L mol}^{-1}$ ,  $K_1 = 1.5986 \text{ L mol}^{-1}$ . The details of the derivation and solution of the Langmuir–Hinshelwood model for the catalyst system are provided in Amoo's thesis in Ref. [34].

To determine activation parameters for the methanolysis of ammonia borane catalysed by Co–Ni–P/Pd– $\text{Al}_2\text{O}_3$  nanoparticles, a series of experiments were performed at various temperatures in the range 30–55 °C, keeping the concentration of the substrate AB at 100 mM (31.5 mg), and the amount of Co–Ni–P/Pd– $\text{Al}_2\text{O}_3$  catalyst at 31.5 mg. The composition ratios of Co–Ni–P/Pd– $\text{Al}_2\text{O}_3$  used for this experiment were [Co–Ni (0:100)], [Co–Ni (50:50)], and [Co–Ni (100:0)]. Fig. 9(a–c) illustrate the plot of the mole of  $\text{H}_2$  evolved per mole of  $\text{H}_3\text{NBH}_3$  from the methanolysis of AB solution versus time in the presence of the three (3) Co–Ni–P/Pd– $\text{Al}_2\text{O}_3$  catalyst types at various temperatures. As expected, the rate of hydrogen generation from the methanolysis of ammonia borane increases with increasing temperature. The observed experimental rate constants (Table 2) for the catalytic methanolysis of ammonia borane at different temperatures were calculated from the linear part of each plot given in Fig. 9(a–c).

The data was used for the construction of Arrhenius [35] and Eyring [36] plots depicted in Fig. 10(a) and (b), respectively, from which the activation parameters shown in Table 3 were determined.

The activation energies for the hydrogen generation from the methanolysis of AB catalysed by the Co–Ni (0:100), Co–Ni (50:50), and Co–Ni (100:0) are comparable to the literature values reported for the methanolysis of AB using different metal containing catalysts (Table 4) [37–42].

The results indicate that 100% Co has the lowest activation energy value at  $33.5 \text{ kJ mol}^{-1}$ ; a value comparable to that of Pd and Ru shown in Table 4. As shown in Table 3, the kinetic parameters of the methanolysis of AB changed with varying Co–Ni compositions in the bath. However, a comparison of the initial Co–Ni composition in the electroless bath with the deposited Co–Ni–P catalyst composition shown in Table 5 indicates that Co–Ni ratio in the catalyst deposit is about the same as their ratio in the starting electroless bath. The results can be used to correlate and estimate the kinetic parameters of any given Co–Ni catalyst composition using the same electroless bath plating conditions. For example, at 30 °C (using data from the present work), the kinetic rate constant for any electroless Co–Ni catalyst composition is given as

$$k_{\text{cor}} = (0.178\text{Co}^{2.14} + 0.006892) \frac{\text{mol}}{\text{g-cat. s}}$$

here, Co is the fraction of the Cobalt in the deposit. For instance, the Co–Ni (86.4:13.6) catalyst, based on the above correlation will have a kinetic rate constant given by  $k_{\text{cor}} = 0.1371 \frac{\text{mol}}{\text{g-cat. s}}$  (cf. the rate constant for cobalt under same conditions is  $0.1849 \frac{\text{mol}}{\text{g-cat. s}}$ ). Similar correlations can be made for  $E_a$  and other kinetic parameters.

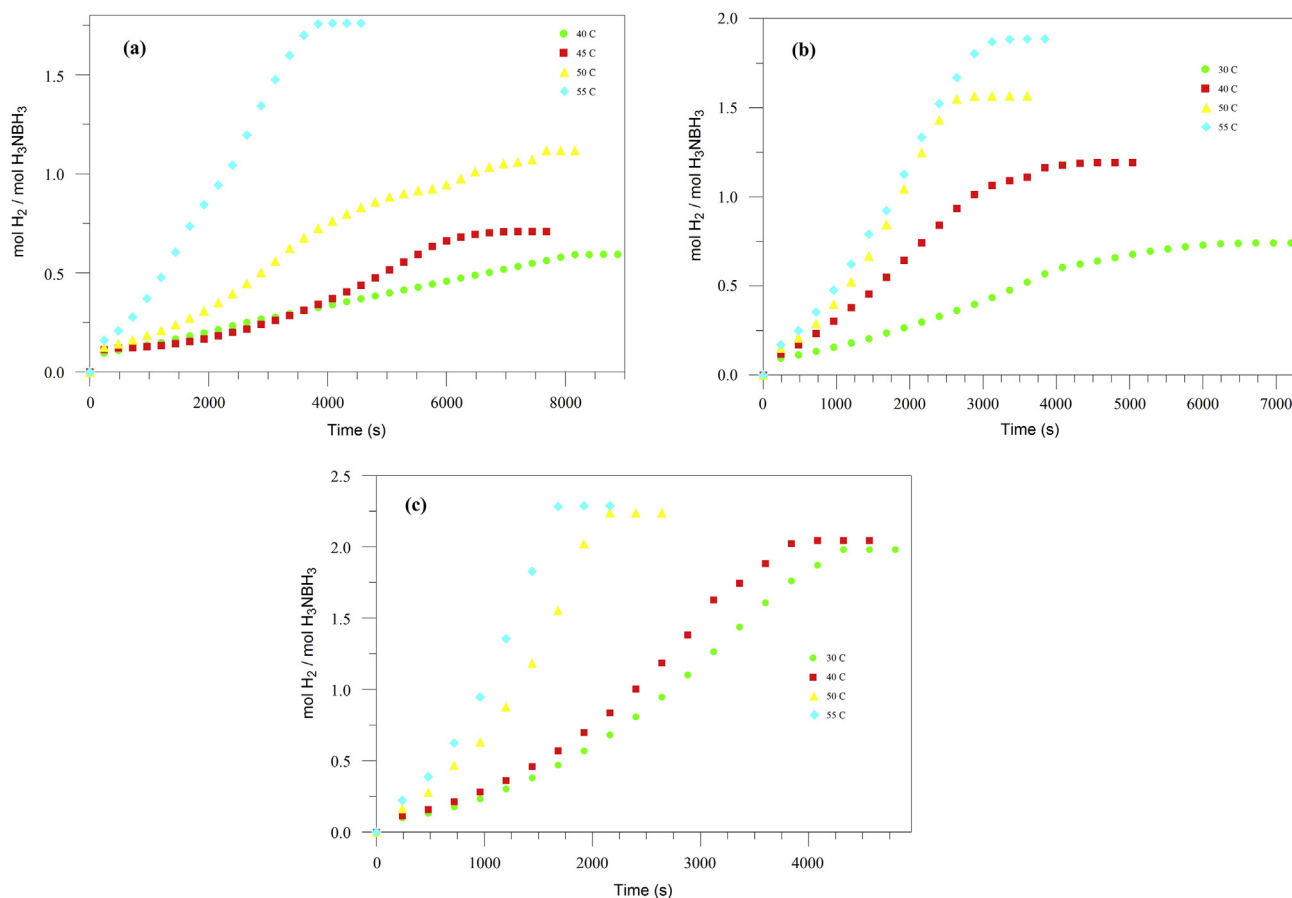


**Fig. 9 – Plots of mol H<sub>2</sub> evolved per mol of H<sub>3</sub>NBH<sub>3</sub> versus time (s) for the catalytic methanolysis of AB (31.5 mg, 100 mM) catalysed by (a) Co–Ni–P/Pd–Al<sub>2</sub>O<sub>3</sub> (0:100) catalyst (31.5 mg), temperature range 40–55 °C, (b) Co–Ni–P/Pd–Al<sub>2</sub>O<sub>3</sub> (50:50) catalyst (31.5 mg), temperature range 30–55 °C, and (c) Co–Ni–P/Pd–Al<sub>2</sub>O<sub>3</sub> (100:0) catalyst (31.5 mg), temperature range 40–55 °C.**

#### Reusability test of the Co–Ni–P/Pd–Al<sub>2</sub>O<sub>3</sub> catalyst

The reusability of the Co–Ni–P/Pd–Al<sub>2</sub>O<sub>3</sub> catalyst is fundamental in the practical H<sub>2</sub> generation apparatus. In the current study, the Co–Ni–P catalyst whose composition was chosen based on its closeness to the properties of pure cobalt (Co–Ni ratio of (86.4:13.6)) was tested for its isolability and reusability in the methanolysis of ammonia-borane. After the

catalytic dehydrogenation reaction of AB was completed, the used catalyst was separated from the solution through filtration, washed thoroughly with deionized water and methanol, then dried in the oven at 60 °C, and reused in the methanolysis of ammonia-borane (15.75 mg, 50 mM). A fresh equivalent of aqueous AB concentration of 50 mM was always added to the reactor vessel for each reusability test. The reusability experiments were carried out at a temperature of 40 °C and repeated 5 times under atmospheric pressure. As seen in Fig. 11, the Co–Ni–P/Pd–Al<sub>2</sub>O<sub>3</sub> (Co–Ni 86.4:13.6) catalyst retains 65% of its initial activity after a series of repeated methanolysis reaction of H<sub>3</sub>NBH<sub>3</sub>, isolation, and re-dispersion cycles at 40 ± 0.5 °C; up to the fifth cycle, releasing the same amount of H<sub>2</sub> gas as the first cycle. This indicates that the Co–Ni–P/Pd–Al<sub>2</sub>O<sub>3</sub> (Co–Ni 86.4:13.6) catalyst is isolable, re-dispersible and yet catalytically active. However, the gradual decrease in the catalytic activity in the subsequent cycles may be attributed to the passivation of the catalyst surface by the increasing concentration of boron products, e.g. NH<sub>4</sub>B(OCH<sub>3</sub>)<sub>4</sub>, which decreases the accessibility of active sites [43], or to the loss of catalyst during isolation processes after previous runs.

**Table 2 – The values of experimental rate constant  $k'$ , for the catalytic methanolysis of AB starting with a solution of 31.5 mg (100 mM) AB and 31.5 mg Co–Ni–P/Pd–Al<sub>2</sub>O<sub>3</sub> catalysts (0:100, 50:50, and 100:0) at different temperatures.**

Temperature (K)	Rate constant (mol H <sub>2</sub> (g <sub>catalyst</sub> ) <sup>−1</sup> (s) <sup>−1</sup> )		
	Co–Ni (0:100)	Co–Ni (50:50)	Co–Ni (100:0)
303.15	–	0.043024	0.19138
313.15	0.025221	0.103852	0.24183
318.15	0.038574	–	–
323.15	0.056377	0.206221	0.40799
328.15	0.175065	0.224024	0.51629

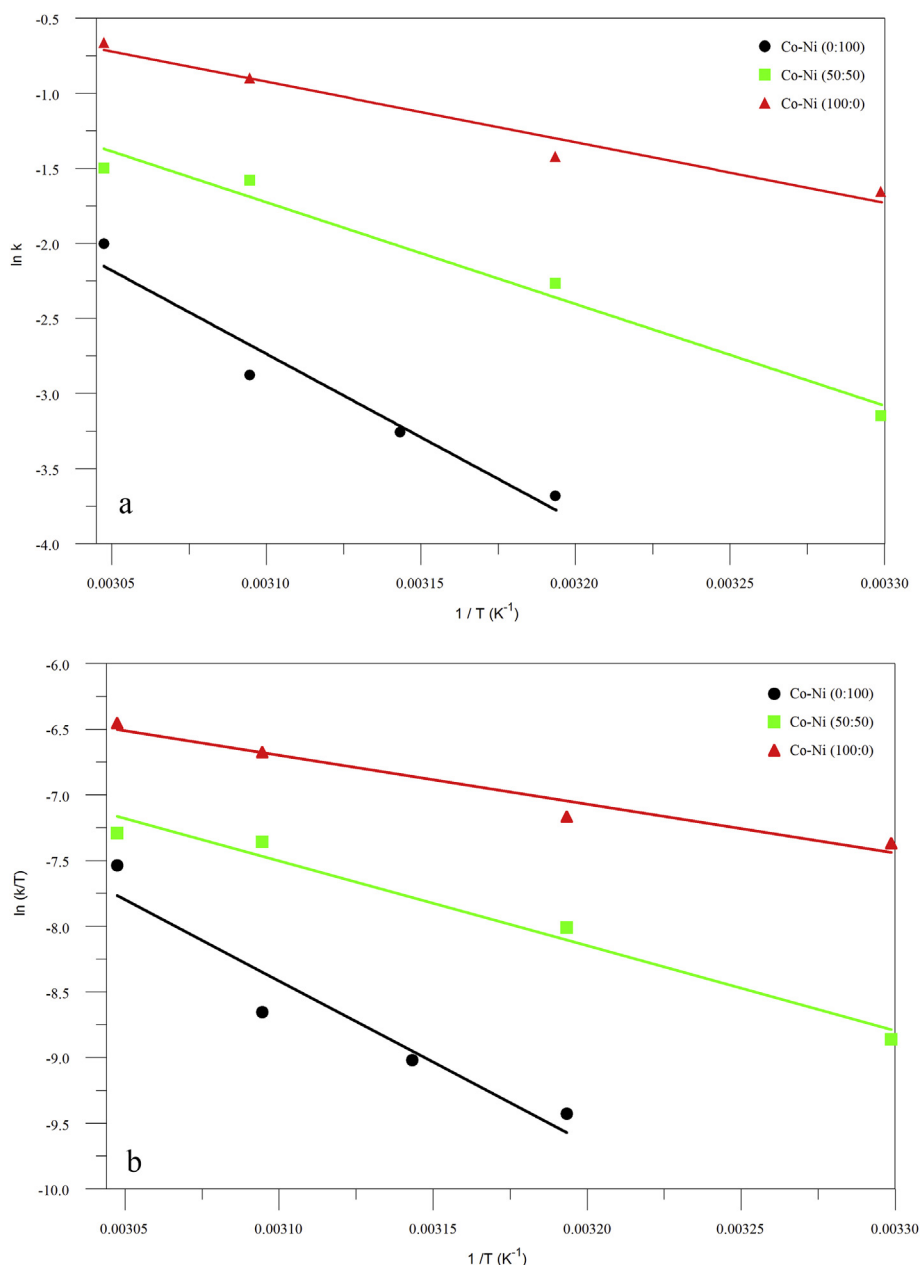


Fig. 10 – a) Arrhenius plots ( $\ln k$  versus the reciprocal of absolute temperature  $1/T$  ( $K^{-1}$ )) for the catalytic methanolysis of AB catalysed by Co–Ni–P/Pd– $Al_2O_3$  (0:100), (50:50) and (100:0) catalyst nanoparticles. b) Eyring plots ( $\ln(k/T)$  versus the reciprocal of absolute temperature  $1/T$  ( $K^{-1}$ )) for the catalytic methanolysis of AB catalysed by Co–Ni–P/Pd– $Al_2O_3$  (0:100), (50:50) and (100:0) catalyst nanoparticles.

**Table 3 – Compared values of the kinetic parameters of the catalytic methanolysis of  $H_2NBH_3$  using different ratios of the Co–Ni–P/Pd– $Al_2O_3$  catalyst particles.**

Parameters	Co–Ni–P/Pd– $Al_2O_3$ catalyst particles		
	Co–Ni (0:100)	Co–Ni (50:50)	Co–Ni (100:0)
$E_a$ ( $kJ\ mol^{-1}$ )	92.4	56.3	33.5
$\Delta H$ ( $kJ\ mol^{-1}$ )	102.7	53.7	30.9
$\Delta S$ ( $J/K\ mol$ )	–50.96	–93.37	–157.38
$A$ ( $mol\ s^{-1}gcat^{-1}$ )	$5.86 \times 10^{13}$	$2.4 \times 10^8$	$1.1 \times 10^5$

## Conclusions

In conclusion, major findings of this research work on the preparation and characterization of the Co–Ni–P/Pd– $Al_2O_3$  catalyst nanoparticles, and evaluation of its catalytic activity in the generation of hydrogen from the catalytic methanolysis of ammonia-borane, can be summarized as follows:

- The Co–Ni–P/Pd– $Al_2O_3$  catalysts were prepared by the electroless deposition of cobalt and nickel metal



**Table 4 – Activation energy values for various reported metal catalysts used for the catalytic methanolysis of ammonia borane.**

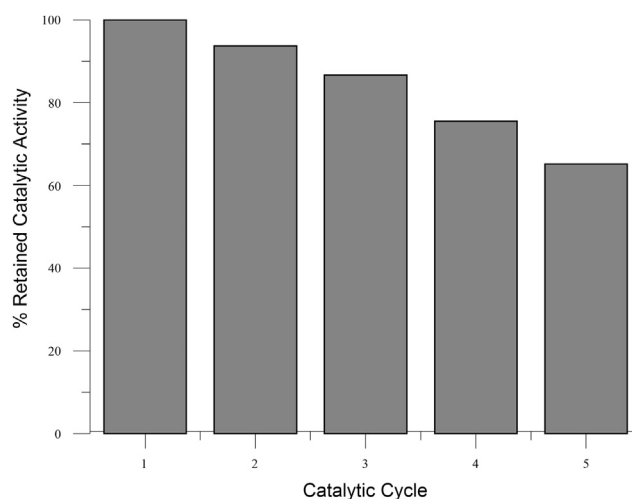
Catalyst	Temp (°C)	E <sub>a</sub> (kJ mol <sup>-1</sup> )	Ref.
Nano PVP-Pd	25	35	[10]
Nano PVP-Ru	25	58	[11]
Mesoporous CuO	25	34.2 ± 1.2	[37]
Nano PVP-Ni	25	62	[38]
Ru/MMT	25	23.8	[39]
Cu–Cu <sub>2</sub> O–CuO/C	30	67.9	[40]
Rh(O)/nano SiO <sub>2</sub>	25	62 ± 2	[41]
G6-OH(Pd <sub>160</sub> )	25	17.9	[42]
Co–Ni (0:100)	40	92.4	This work
Co–Ni (50:50)	30	56.3	This work
Co–Ni (100:0)	30	33.5	This work

**Table 5 – A comparison of Co–Ni atomic ratio in the starting electroless bath versus their ratio in the deposited Co–Ni–P catalyst. The atomic ratio of the deposit with the co-deposited phosphorus is included in parenthesis.**

Catalyst	Electroless bath atomic ratio	EDS atomic ratio
Co–Ni (0:100)	Ni	Ni
Co–Ni (33.3:66.7)	Co <sub>0.5</sub> Ni <sub>1</sub>	Co <sub>0.6</sub> Ni <sub>1</sub> (Co <sub>7</sub> Ni <sub>11</sub> P <sub>1</sub> )
Co–Ni (50:50)	Co <sub>1</sub> Ni <sub>1</sub>	Co <sub>1</sub> Ni <sub>1</sub> (Co <sub>15</sub> Ni <sub>15</sub> P <sub>1</sub> )
Co–Ni (66.7:33.3)	Co <sub>2</sub> Ni <sub>1</sub>	Co <sub>1.6</sub> Ni <sub>1</sub> (Co <sub>14</sub> Ni <sub>9</sub> P <sub>1</sub> )
Co–Ni (86.37:13.63)	Co <sub>6</sub> Ni <sub>1</sub>	Co <sub>9</sub> Ni <sub>1</sub> (Co <sub>28</sub> Ni <sub>3</sub> P <sub>1</sub> )
Co–Ni (100:0)	Co	Co

particles on the polymer-stabilized palladium nanoparticle-activated aluminium-oxide substrate support after a plating time of 30 min. These catalysts can be isolated by filtration and thorough washing from the electroless bath solution.

- ii. The atomic ratio of Co–Ni in the deposited electroless catalyst was the same as their atomic ratios in the initial electroless bath.
- iii. The Co–Ni–P/Pd–Al<sub>2</sub>O<sub>3</sub> catalyst types were characterized using X-ray Diffraction (XRD), Energy Dispersive X-ray Spectroscopy (EDS) and Scanning Electron Microscopy (SEM) techniques. The results revealed that the Co–Ni alloy particles were indeed deposited on the surface of the Pd-activated Al<sub>2</sub>O<sub>3</sub> support.
- iv. The results gotten from the kinetic study show that the catalytic methanolysis reaction of ammonia-borane is of order 0.83 with respect to the catalyst weight and zero order with respect to ammonia-borane concentration when the catalyst is treated just as a reactant instead of as a heterogeneous catalyst.
- v. We demonstrated that the rate determining step in the catalytic methanolysis of ammonia borane is the hydrogen desorption step. The kinetic parameters were obtained from the Langmuir–Hinshelwood kinetic model.
- vi. Thermodynamic parameters, such as  $\Delta H$ ,  $\Delta S$ ,  $A$  and  $E_a$  were also successfully derived from both the Eyring and Arrhenius equations for the Co–Ni–P/Pd–Al<sub>2</sub>O<sub>3</sub> nanoparticles. The order of enthalpy of activation ( $\Delta H$ ) ( $\Delta H_{(0:100)} > \Delta H_{(50:50)} > \Delta H_{(100:0)}$ ) were well-correlated with

**Fig. 11 – % Retained catalytic activity versus number of subsequent catalytic cycles for Co–Ni 86.4:13.6 (31.5 mg) catalysed methanolytic dehydrogenation of H<sub>3</sub>NBH<sub>3</sub> (15.75 mg, 50 mM) at 40 ± 0.5 °C.**

the order of activation energy ( $E_a$ ) ( $E_{a(0:100)} > E_{a(50:50)} > E_{a(100:0)}$ ).

- vii. The thermodynamic and kinetic rate parameters can be correlated with the composition ratios of Co–Ni used in the electroless deposition.
- viii. The release of hydrogen gas during the reusability test (performed by dispersing the catalysts isolated after each run) showed that the volume of hydrogen released at successive runs was still the same even at the fifth cycle. Thus, the catalysts are isolable, re-dispersible and reusable. When re-dispersed in the aqueous ammonia-borane solution, the Co–Ni–P/Pd–Al<sub>2</sub>O<sub>3</sub> (Co–Ni 86.4:13.6) catalyst retains 65% of its initial activity.
- ix. The high catalytic activity, stability, relatively easy preparation, reusability and economical cost make the Co–Ni–P/Pd–Al<sub>2</sub>O<sub>3</sub> (Co–Ni 86.4:13.6) catalyst a promising candidate to be used as catalyst in developing highly efficient portable hydrogen generation system based on methanolysis reaction using ammonia-borane as a solid hydrogen storage material.

## Acknowledgements

We thank Carnegie ADF for Fellowship (E. E. Kalu) and for partial support by ERC Program of the National Science Foundation under Award Number EEC-08212121.

## Nomenclature

$k'$	experimental rate constant, mol H <sub>2</sub> (g-catalyst) <sup>-1</sup> (s) <sup>-1</sup>
$k_{H_2}$	surface rate constant, mol mg <sup>-1</sup> s <sup>-1</sup>
$K_{H_2}$	desorption equilibrium constant of H <sub>2</sub> , L mol <sup>-1</sup>
$K_1$	overall equilibrium constant, L mol <sup>-1</sup>
$\Delta H$	enthalpy of activation, kJ mol <sup>-1</sup>

$\Delta S$	entropy of activation, $\text{J mol}^{-1} \text{K}^{-1}$
A	pre-exponential factor, $\text{mL s}^{-1} (\text{g-catalyst})^{-1}$
E <sub>a</sub>	activation energy, $\text{kJ mol}^{-1}$
$r_{\text{D,H}_2}$	rate of desorption of hydrogen controlling, $\text{mol H}_2 (\text{g-catalyst})^{-1} (\text{s})^{-1}$
C <sub>A</sub>	concentration of ammonia-borane, mM
C <sub>B</sub>	concentration of methanol, mM
C <sub>C</sub>	concentration of ammonium tetramethoxyborate, mM

## REFERENCES

- [1] Hausdorf S, Baitalow F, Wolf G, Mertens FO. A procedure for the regeneration of ammonia borane from BNH-waste products. *Int J Hydrogen Energy* 2008;33(Pt 2):608–14.
- [2] Ramachandran PV, Gagare PD. Preparation of ammonia borane in high yield and purity, methanolysis, and regeneration. *Inorg Chem* 2007;46(Pt 19):7810–7.
- [3] Stephens FH, Pons V, Baker RT. Ammonia–borane: the hydrogen source par excellence? *Dalton Trans* 2007;25:2613–26.
- [4] Chandra M, Xu Q. A high-performance hydrogen generation system: transition metal-catalyzed dissociation and hydrolysis of ammonia–borane. *J Power Sources* 2006;156(Pt 2):190–4.
- [5] Kang K, Gu X, Guo L, Liu P, Sheng X, Wu Y, et al. Efficient catalytic hydrolytic dehydrogenation of ammonia borane over surfactant-free bimetallic nanoparticles immobilized on amine-functionalized carbon nanotubes. *Int J Hydrogen Energy* 2015;40:12315–24.
- [6] Wang H, Zhou L, Han M, Tao Z, Cheng F, Chen J. CuCo nanoparticles supported on hierarchically porous carbon as catalysts for hydrolysis of ammonia borane. *J Alloys Comp* 2015;651:382–8.
- [7] Xiong X, Zhou L, Yu G, Yang K, Ye M, Xia Q. Synthesis and catalytic performance of a novel RuCuNi/CNTs nanocomposite in hydrolytic dehydrogenation of ammonia borane. *Int J Hydrogen Energy* 2015;40:15521–8.
- [8] Zhang H, Wang X, Chen C, An C, Xu Y, Huang Y. Facile synthesis of Cu@CoNi core-shell nanoparticles composites for the catalytic hydrolysis of ammonia borane. *Int J Hydrogen Energy* 2015;40:12253–61.
- [9] Rakap M. PVP-stabilized Ru-Rh nanoparticles as highly efficient catalysts for hydrogen generation from hydrolysis of ammonia borane. *J Alloys Comp* 2015;649:1025–30.
- [10] Erdoğan H, Metin Ö, Özkar S. In situ-generated PVP-stabilized palladium (0) nanocluster catalyst in hydrogen generation from the methanolysis of ammonia–borane. *Phys Chem Chem Phys* 2009;11(Pt 44):10519–25.
- [11] Erdoğan H, Metin Ö, Özkar S. Hydrogen generation from the methanolysis of ammonia borane catalyzed by in situ generated, polymer stabilized ruthenium (0) nanoclusters. *Catal Today* 2011;170(Pt 1):93–8.
- [12] Çalışkan S, Zahmakıran M, Özkar S. Zeolite confined rhodium (0) nanoclusters as highly active, reusable, and long-lived catalyst in the methanolysis of ammonia-borane. *Appl Catal B Environ* 2010;93(Pt 3):387–94.
- [13] Brown HC, Brown CA. New, highly active metal catalysts for the hydrolysis of borohydride. *J Am Chem Soc* 1962;84(Pt 8):1493–4.
- [14] Kojima Y, Suzuki KI, Fukumoto K, Sasaki M, Yamamoto T, Kawai Y, et al. Hydrogen generation using sodium borohydride solution and metal catalyst coated on metal oxide. *Int J Hydrogen Energy* 2002;27(Pt 10):1029–34.
- [15] Wu C, Zhang H, Yi B. Hydrogen generation from catalytic hydrolysis of sodium borohydride for proton exchange membrane fuel cells. *Catal Today* 2004;93:477–83.
- [16] Chou C-C, Chen B-H. Hydrogen generation from deliquescence of ammonia borane using Ni-Co/r-GO catalyst. *J Power Sources* 2015;293:343–50.
- [17] Krishnan P, Yang TH, Lee WY, Kim CS. PtRu–LiCoO<sub>2</sub>—an efficient catalyst for hydrogen generation from sodium borohydride solutions. *J Power Sources* 2005;143(Pt 1):17–23.
- [18] Wee JH, Lee KY, Kim SH. Sodium borohydride as the hydrogen supplier for proton exchange membrane fuel cell systems. *Fuel Process Tech* 2006;87(Pt 9):811–9.
- [19] Schlesinger HI, Brown HC, Finholt AE, Gilbreath JR, Hoekstra HR, Hyde EK. Sodium borohydride, its hydrolysis and its use as a reducing agent and in the generation of hydrogen. *J Am Chem Soc* 1953;75(Pt 1):215–9.
- [20] Lee J, Kong KY, Jung CR, Cho E, Yoon SP, Han J, et al. A structured Co–B catalyst for hydrogen extraction from NaBH<sub>4</sub> solution. *Catal Today* 2007;120(Pt 3):305–10.
- [21] Sun D, Mazumder V, Metin O, Sun S. Methanolysis of ammonia borane by CoPd nanoparticles. *ACS Catal* 2012;2(Pt 6):1290–5.
- [22] Kalidindi SB, Vernekar AA, Jagirdar BR. Co–Co<sub>2</sub>B, Ni–Ni<sub>3</sub>B and Co–Ni–B nanocomposites catalyzed ammonia–borane methanolysis for hydrogen generation. *Phys Chem Chem Phys* 2009;11(Pt 5):770–5.
- [23] Zahmakıran M, Özkar S. Metal nanoparticles in liquid phase catalysis; from recent advances to future goals. *Nanoscale* 2011;3(Pt 9):3462–81.
- [24] El-Shall MS, Abdelsayed V, Abd El Rahman SK, Hassan HM, El-Kaderi HM, Reich TE. Metallic and bimetallic nanocatalysts incorporated into highly porous coordination polymer MIL-101. *J Mater Chem* 2009;19(Pt 41):7625–31.
- [25] Foxx D, Kalu EE. Amperometric biosensor based on thermally activated polymer-stabilized metal nanoparticles. *Electrochem Comm* 2007;9(Pt 4):584–90.
- [26] Kuruganti AS, Chen KS, Kalu EE. Tapping mode atomic force microscopy analysis of a novel catalyzed technique on nonconducting substrates. *Electrochem solid-state Lett* 1999;2(Pt 1):27–9.
- [27] Basu S, Brockman A, Gagare P, Zheng Y, Ramachandran PV, Delgass WN, et al. Chemical kinetics of Ru-catalyzed ammonia borane hydrolysis. *J Power Sources* 2009;188(Pt 1):238–43.
- [28] Rakap M, Kalu EE, Özkar S. Hydrogen generation from the hydrolysis of ammonia borane using cobalt-nickel-phosphorus (Co–Ni–P) catalyst supported on Pd-activated TiO<sub>2</sub> by electroless deposition. *Int J Hydrogen Energy* 2011;36(Pt 1):254–61.
- [29] Rakap M, Kalu EE, Özkar S. Hydrogen generation from hydrolysis of ammonia-borane using Pd–PVB–TiO<sub>2</sub> and Co–Ni–P/Pd–TiO<sub>2</sub> under stirred conditions. *J Power Sources* 2012;210:184–90.
- [30] Yao Q, Lu ZH, Jia Y, Chen X, Liu X. In situ facile synthesis of Rh nanoparticles supported on carbon nanotubes as highly active catalysts for H<sub>2</sub> generation from NH<sub>3</sub>BH<sub>3</sub> hydrolysis. *Int J Hydrogen Energy* 2015;40(Pt 5):2207–15.
- [31] Zou Y, Cheng J, Wang Q, Xiang C, Chu H, Qiu S, et al. Cobalt–boron/nickel–boron nanocomposite with improved catalytic performance for the hydrolysis of ammonia borane. *Int J Hydrogen Energy* 2015;40(Pt 39):13423–30.
- [32] Özhava D, Özkar S. Rhodium (0) nanoparticles supported on hydroxyapatite nanospheres and further stabilized by dihydrogen phosphate ion: a highly active catalyst in hydrogen generation from the methanolysis of ammonia borane. *Int J Hydrogen Energy* 2015;40(Pt 33):10491–501.
- [33] Peng S, Liu J, Zhang J, Wang F. An improved preparation of graphene supported ultrafine ruthenium (0) NPs: very active and durable catalysts for H<sub>2</sub> generation from methanolysis

- of ammonia borane. *Int J Hydrogen Energy* 2015;40(Pt 34):10856–66.
- [34] Amoo KO. Hydrogen generation from the methanolysis of ammonia-borane using cobalt-nickel-phosphorus (Co-Ni-P) catalyst supported on Pd-Activated  $\text{Al}_2\text{O}_3$  by electroless deposition (MS thesis). Covenant University; 2016.
- [35] Laidler KJ. Chemical kinetics. 3rd. ed. New York: Harper & Row Publishers; 1987.
- [36] Eyring H. The activated complex in chemical reactions. *J Chem Phys* 1935;3(Pt 2):107–15.
- [37] Yao Q, Huang M, Lu ZH, Yang Y, Zhang Y, Chen X, et al. Methanolysis of ammonia borane by shape-controlled mesoporous copper nanostructures for hydrogen generation. *Dalton Trans* 2015;44(Pt 3):1070–6.
- [38] Özhava D, Kılıçaslan NZ, Özkar S. PVP-stabilized nickel (0) nanoparticles as catalyst in hydrogen generation from the methanolysis of hydrazine borane or ammonia borane. *Appl Catal B Environ* 2015;162:573–82.
- [39] Dai HB, Kang XD, Wang P. Ruthenium nanoparticles immobilized in montmorillonite used as catalyst for methanolysis of ammonia borane. *Int J Hydrogen Energy* 2010;35(Pt 19):10317–23.
- [40] Yurderi M, Bulut A, Ertas IE, Zahmakiran M, Kaya M. Supported copper-copper oxide nanoparticles as active, stable and low-cost catalyst in the methanolysis of ammonia-borane for chemical hydrogen storage. *Appl Catal B Environ* 2015;165:169–75.
- [41] Özhava D, Özkar S. Rhodium (0) nanoparticles supported on nanosilica: highly active and long lived catalyst in hydrogen generation from the methanolysis of ammonia borane. *Appl Catal B Environ* 2016;181:716–26.
- [42] Noh JH, Meijboom R. Catalytic evaluation of dendrimer-templated Pd nanoparticles in the reduction of 4-nitrophenol using Langmuir–Hinshelwood kinetics. *Appl Surf Sci* 2014;320:400–13.
- [43] Jaska CA, Clark TJ, Clendenning SB, Grozea D, Turak A, Lu ZH, et al. Poisoning of heterogeneous, late transition metal dehydrocoupling catalysts by boranes and other group 13 hydrides. *J Am Chem Soc* 2005;127(Pt 14):5116–24.